Spectral kinks and mid-infrared optical conductivity of doped Mott insulators from strong electron correlations

Shiladitya Chakraborty, Dimitrios Galanakis, and Philip Phillips
Department of Physics, University of Illinois, 1110 W. Green Street, Urbana, Illinois 61801, USA
(Received 29 April 2008; published 16 December 2008)

We compute the one-particle spectral function and the optical conductivity for the two-dimensional Hubbard model on a square lattice. The computational method is cellular dynamical mean-field theory in which a four-site Hubbard plaquette is embedded in a self-consistent bath. We obtain a "kink" feature in the dispersion of the spectral function and a mid-infrared (mid-IR) absorption peak in the optical conductivity, consistent with experimental data. Of the 256 plaquette states, only a single state which has $d_{x^2-y^2}$ symmetry contributes to the mid-IR, thereby suggesting a direct link with the pseudogap. Local correlations between doubly and singly occupied sites which lower the kinetic energy of a hole are the efficient cause of this effect.

DOI: 10.1103/PhysRevB.78.212504 PACS number(s): 74.25.Gz, 72.80.−r, 74.20.−z, 74.25.Fy

A distinctive feature seen in angle-resolved photoemission spectroscopy (ARPES) spectra on the high-temperature copper oxide superconductors (cuprates) is the kink[1] or abrupt change in the slope of the electron dispersion ω vs k. The abrupt change in the slope in the electron dispersion or the quasiparticle velocity obtained from ARPES has been observed in various families of hole-doped cuprates at an energy of 50–80 meV. The size of the kink decreases with hole doping x and the kink seems to disappear around $x=0.3$. Since ARPES offers a direct measure of the spectral function, the imaginary part of the self-energy can also be deduced. Experimentally, the imaginary part of the self-energy $\mathrm{Im}\,\Sigma(k,\omega)$ shows a suppression, indicating a diminished scattering rate,[2] at the kink energy. The presence of the kink is reminiscent of similar observations in the spectra of conventional BCS superconductors, where phonons cause an abrupt change in the electron dispersion as well. Consequently, explanations based on collective phonon excitations[1,3–8] have been invoked to explain the ubiquitous kink feature. Rival explanations include purely electronic scenarios based on spin fluctuations.[9,10] Recent ARPES experiments[11,12] find that kink phenomena occur at high energies as well. At the high-energy kink (referred to colloquially as the waterfall), the electron dispersion bifurcates.

Equally striking is the optical conductivity in the mid-infrared (mid-IR). The optical conductivity of a material can be extracted from its measured reflectivity $R(\omega)$ spectrum using the Kramers-Kronig (KK) relations.[13–15] Two universal features seen in the optical conductivity of the cuprates are (1) a Drude peak at low energies followed by (2) an absorption feature in the mid-IR region. The Drude peak corresponds to the motion of free carriers in the system for which the Drude model predicts a conductivity peak at zero frequency. The existence of an absorption feature in the mid-IR region is unexpected since doped Mott insulators are expected to have spectral weight either at the high-energy sector across the Mott gap (UV) or at low energy, close to the Fermi level (far IR).[16] The spectral weight of the mid-IR band in the optical conductivity is an increasing[14,17–20] function of doping whereas the band at high energy (UV) decreases. This trade-off suggests that the origin of the mid-IR band (MIB) arises fundamentally from the strong correlations that mediate the Mott state. It is not surprising then that no low-T_c materials exhibit a MIB in their optical conductivity. Amidst the myriad explanations proposed,[21–27] none has emerged as the definitive answer to this problem.

In a series of recent papers[28–30] we formulated the exact low-energy theory of a doped Mott insulator and showed that another excitation emerges at low energies. The excitation is a charge $2e$ boson which is not made out of elemental excitations. This excitation was shown to offer a unifying mechanism for the kink features (both high and low energies as well as the bifurcation of the electron dispersion) and the mid-IR band. What we present here is a series of numerical studies on the Hubbard model which offers an independent test of the predictions of the low-energy theory. To this end, we employ the state-of-the-art numerical method on the Hubbard model, cellular dynamical mean-field theory (CDMFT),[31] to investigate whether the low-energy kink and mid-IR bands have purely electronic origins. We find that both the kink and the mid-IR are linked to short-range electronic correlations. In particular, the mid-IR arises from a mixing of the upper and lower Hubbard bands through an electronic state that has $d_{x^2-y^2}$ symmetry, suggesting that the pseudogap is also due to the same mechanism. This mechanism is identical to that mediated by the charge $2e$ boson in the exact low-energy theory.

To this end, we start with the two-dimensional (2D) Hubbard model,

$$H_{\mathrm{Hubbard}} = -t\sum_{i,j,\sigma} g_{ij} c^{\dagger}_{i,\sigma} c_{j,\sigma} + U\sum_{i,\sigma} c^{\dagger}_{i,\uparrow} c^{\dagger}_{i,\downarrow} c_{i,\downarrow} c_{i,\uparrow}. \qquad (1)$$

Here i,j label lattice sites, g_{ij} is equal to 1 if i,j are nearest neighbors, $c_{i\sigma}$ annihilates an electron with spin σ on lattice site i, t is the nearest-neighbor hopping matrix element, and U the energy cost when two electrons doubly occupy the same site. The cuprates live in the strongly coupled regime in which the interactions dominate as $t \approx 0.5$ eV and $U=4$ eV. Various numerical techniques have been developed to study strongly interacting systems on a lattice. These include exact diagonalization (Lanczos technique), quantum Monte Carlo, and cluster methods. In this study, we use cluster dynamical mean-field theory[32] to compute the one-

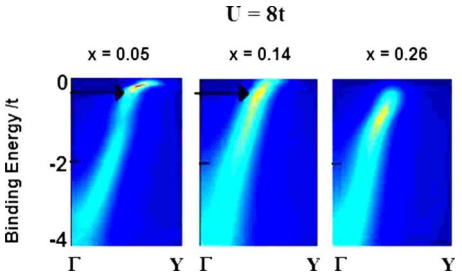

FIG. 1. (Color online) Intensity plot of the spectral function computed along the nodal $\Gamma=(0,0)\rightarrow Y=(\pi,\pi)$ direction for $U=8t$ at three different hole dopings. The arrows in the first two panels indicate the position of the kink.

particle Green's function. In this method, we consider exactly the dynamics on a four-site (plaquette) cluster and treat the rest of the lattice as a bath whose degrees of freedom are integrated over. The coupling of the cluster to the bath is thus treated in a mean-field fashion and the cluster quantities are evaluated self-consistently using the cumulant lattice reconstruction scheme.[33] While no variational principle exists for this method, several tests in limiting cases in which the answers are known exactly have revealed that the local correlations that the CDMFT method builds in provide an adequate starting point for quantifying the physics of strong correlations.

Using the CDMFT method, we obtained the one-particle spectral function $A(\mathbf{k},\omega)$ for various values of hole doping x and on-site Coulomb repulsion U (expressed in units of the nearest-neighbor hopping integral t). Hole dopings in the range of 0.03 (lightly doped Mott insulator) up to around 0.30 (heavily overdoped superconductor) have been considered together with a maximum U value of $12t$. Typical spectral functions $A(\mathbf{k},\omega)$ obtained from CDMFT are displayed in three panels in Fig. 1. We have plotted here only the spectral function intensity for different hole dopings in which the brightness at each point $(\mathbf{k},\omega)$ is indicative of the magnitude of $A(\mathbf{k},\omega)$ at that point. The bright band in each panel is the region of maximum $A(\mathbf{k},\omega)$ and defines the ω vs $\mathbf{k}$ dispersion curve. The most interesting feature in these plots is the presence of a distinct kink in the dispersion curve at low doping values and an absence of the kink at the highest doping. The overall doping dependence is in rough agreement with the experimental trends. Also shown in Fig. 2 is the U dependence of the kink energy for three $U=4t$, $U=8t$, and $U=12t$. As seen in Fig. 2, the kink energy scales inversely with U. Fitting the kink energies to $1/U$ gives a very good linear plot with a slope of approximately 4. In other words the kink energy scale is given by $4t^2/U$.

To explore the physics of the kink in further detail, we looked for specific short-range electron correlations within the plaquette that give rise to the kink. Such details are readily available from the 176 local resolvents that comprise the impurity solver method we employed, namely, the noncrossing approximation (NCA). To achieve this, NCA has been selectively employed on various subspaces of the full Hilbert space of the plaquette in order to isolate the effect of each subspace on the spectral function. This requires an extensive search on the $4^4=256$-dimensional Hilbert space and

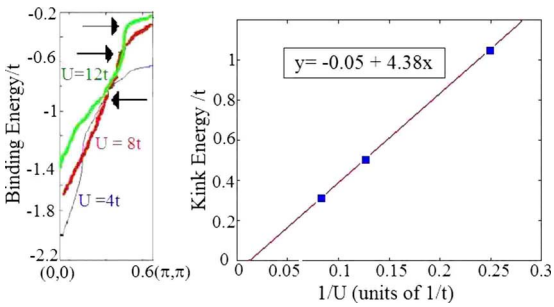

FIG. 2. (Color online) Left panel shows dispersion curves at $x=0.05$ plotted for three different U values with the black arrows showing the position of the kink in each curve. Right panel shows kink energy plotted vs $1/U$ and its linear fit.

isolating the states relevant to kink formation. It turns out that out of 256 plaquette states, only 16 are involved in giving rise to the kink. All of these states (labeled "super-16" in Fig. 3) have four electrons with a total spin $S_z=\pm 1$, i.e., there are three same-spin electrons and an opposite-spin electron on a plaquette. All of the states in the super-16 subspace have some doubly occupied character. By doubly occupied character, we simply mean that there is a nonzero overlap with the doubly occupied sector not that the wave function is predominantly doubly occupied. We also verified that the kink vanishes if the doubly occupied sector is eliminated. Consequently, the kink we have found here does not have a simple interpretation in terms of spin fluctuations as such a scenario would not require the explicitly doubly occupied sector. A kink arising from an explicit mixing between singly and doubly occupied sectors with $S=1$ is consistent, however, with the physics mediated by the charge $2e$ boson[28–30] that appears in the exact low-energy theory of a doped Mott insulator modeled by the Hubbard model. Excitation of the boson, which mediates mixing with all the doubly occupied sectors, occurs on the energy scale t^2/U. Once the boson is excited, the electron dispersion should change. Hence, we conclude that our numerical results are consistent with the physics that the charge $2e$ boson[28,30] mediates at low energy in the Hubbard model.

We also computed the optical conductivity. To obtain a direct link between the conductivity and the spectral func-

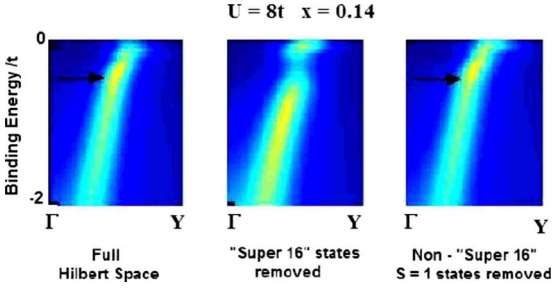

FIG. 3. (Color online) Spectral function for $x=0.14$ obtained in two restricted Hilbert spaces on the plaquette (center and right panels) compared with the complete spectrum (left panel). The kink goes away only when the super-16 states are removed from the Hilbert space and reappears when they are included even when other states with $S_z=\pm 1$ are absent.

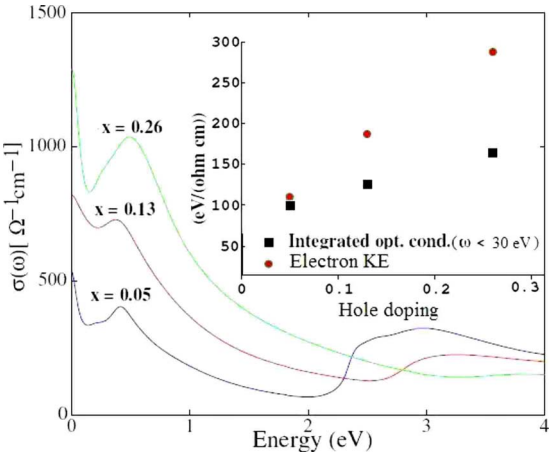

FIG. 4. (Color online) Optical conductivity plots computed using CDMFT for three different hole dopings for $U=8t$, $T=0.1t$. Inset: integrated optical conductivity $K(\Omega)=\int_0^\Omega \sigma(\omega)d\omega$ up to energy of $\Omega=60t=30$ eV (squares) and electron kinetic energy (circles) plotted for three different hole dopings for $U=8t$, $T=0.1t$.

tion, we worked in the noncrossing approximation,

$$\sigma(\omega) = \frac{2e^2}{\nu\hbar^2 N}\sum_{\mathbf{k}} (\nabla_{\mathbf{k}}\epsilon_{\mathbf{k}})^2 \int \frac{d\omega}{2\pi} A(\mathbf{k},\omega') \times A(\mathbf{k},\omega'+\omega)\frac{\mathbf{f}(\omega')-\mathbf{f}(\omega'+\omega)}{\omega}, \quad (2)$$

to the Kubo formula for the conductivity[34–36] where $f(\omega)$ is the Fermi distribution function and $A(\omega,k)$ is the spectral function. Here ν is the unit cell volume and $\epsilon_{\mathbf{k}}$ is the dispersion for the noninteracting system. The optical conductivity has been computed for various dopings and U values. Figure 4 displays the optical conductivity for three different hole dopings. The optical conductivity plots show a peaklike resonance feature (Fig. 4) at 0.5 eV (4000 cm^{-1}) for $U=8t$ which falls right inside the mid-IR region where the experimental[14,17–20] data show an absorption peak. The magnitude of the optical conductivity is also in perfect agreement with experiment.[18,19] The physical origin of this peak can be determined by focusing (see Fig. 5) on the resolvents for states in the plaquette that contribute significantly to the optical conductivity. Surprisingly, of the 256 plaquette states, only a single state in the $N=4$ and $S_z=0$ sector contributes (see Fig. 5) to the mid-IR peak. This state has three key characteristics: (1) it contains a mixture of singly (87%) and doubly occupied (13%) sites, (2) its energy is $-1.3t$, essentially the energy of mid-IR peak, and (3) the spatial symmetry of the eigenstate is $d_{x^2-y^2}$. Any physical process which meets these constraints must also couple to the charge not simply to the spin sector as in the case of antiferromagnetic spin fluctuations. A further hint as to the origin of the MIB is the calculation of Haule and Kotliar[37] indicating that the MIB is absent in the traditional implementation of the t-J model unless superconductivity is present. By traditional implementation, we mean the $U=\infty$ limit in which J is (inconsistently) treated as being finite but double occupancy is excluded in the Hubbard basis rather than being excluded

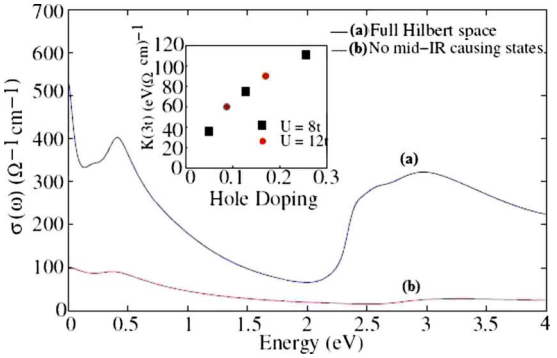

FIG. 5. (Color online) (a) Optical conductivity plot for $U=8t$, $n=0.94$, $T=0.1t$ with distinct mid-IR peak contrasted with (b) the contribution from a restricted Hilbert space with certain $S=0$ states removed. Inset: integrated optical conductivity $K(\Omega)=\int_0^\Omega \sigma(\omega)d\omega$ up to $\Omega=3t=1.5$ eV (restricted f-sum rule) for $U=12t$ and $U=8t$.

only from the transformed basis.[38] The typical process shown in Fig. 6, which is eliminated by imposing the artificial $U=\infty$ constraint, results in the mixing of the high- and low-energy scales by virtue of a hole neighboring a doubly occupied site. This resonance persists even at $x=0$ (although with perhaps vanishing weight) and hence we predict that the restricted f-sum rule at finite doping should extrapolate to a nonzero value at $x=0$ as long as $U\neq\infty$ as depicted in the inset of Fig. 5. As this is the only process through $O(t^2/U)$ that is left out in the $U=\infty$ limit, we conclude that the resonance shown in Fig. 6 is the origin of the mid-IR. This would indicate that the mid-IR is strongly momentum dependent (and hence not adequately described by single-site analyses[39]), having $d_{x^2-y^2}$ symmetry, which is our principal conclusion. That the process in Fig. 6 causes the mid-IR was also the result of our analysis[30] of the exact low-energy theory of the Hubbard model.

An explicit assumption in the NCA procedure [Eq. (2)] is that vertex corrections are not important. That is, the current-current correlator is approximated by the simple bubble diagram and higher-order terms (vertex corrections) are neglected. This approximation is only correct in the limit of infinite dimensions.[40] To determine how valid this approximation is for a $d=2$ system, we computed the kinetic energy explicitly versus the value predicted from the sum rule,

$$K(\infty) = -\frac{\pi e^2 a^2}{2\hbar^2 V} E_{\text{kin}}, \quad (3)$$

where $K(\Omega)=\int_0^\Omega \sigma(\omega)d\omega$ is the integrated optical spectral weight, e is the electron charge, a is the lattice constant, and

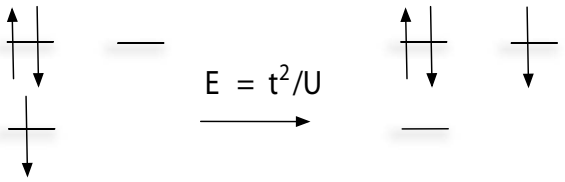

FIG. 6. Hopping process that mixes the upper and lower Hubbard bands that leads to the mid-IR band. This process requires that the hole and the doubly occupied site are neighbors. It is the motion of this bound state that we attribute to the mid-IR band.

V is the volume of the unit cell. This sum rule is expected to hold as long as the hopping terms are mediated by nearest-neighbor hopping processes. The integrated optical conductivity and the electron kinetic energy (computed explicitly using CDMFT) have been plotted for various hole doping levels in the inset of Fig. 4. We find that the sum rule is reasonably well obeyed for low hole dopings ($x=0.05$) near half-filling. However, further away from half-filling where the low-energy sector contains increased spectral weight transferred from high energy, the integrated optical conductivity fails to account for the kinetic energy. This behavior is not unexpected as the vertex corrections ignored in Eq. (2) are strongly doping dependent and hence Eq. (2) is more accurate close to half-filling. As our focus is on the mid-infrared feature, which is most well defined close to half-filling, our treatment here should be adequate.

The key feature that distinguishes this work is the finding that double occupancy mediates both the low-energy kink and the mid-IR band. Our result that the mid-IR is caused by a single state (of the 256 plaquette states) that has $d_{x^2-y^2}$ symmetry is striking and indicates that the mid-IR is likely to be caused by the same physics that underlies the pseudogap as optics experiments seem to indicate.[14] Further, the mechanism identified here, which is identical to that mediated by the charge $2e$ boson in the exact low-energy theory of the Hubbard model[28–30] (Fig. 6), could explain why an extrapolated nonzero intercept of the restricted f-sum rule might be a generic feature of doped Mott insulators, in contrast to recent claims.[39]

We thank A. Millis for sharing with us his DMFT results and for a discussion on the sum rule, G. A. Sawatzky, G. Kotliar, and D. Basov for helpful discussions, and NSF under Grants No. DMR0605769 and No. PHY05-051164 for partially funding this work.

[1] A. Lanzara *et al.*, Nature (London) **412**, 510 (2001).
[2] X. J. Zhou *et al.*, Phys. Rev. Lett. **95**, 117001 (2005).
[3] A. Damascelli *et al.*, Rev. Mod. Phys. **75**, 473 (2003).
[4] P. V. Bogdanov *et al.*, Phys. Rev. Lett. **85**, 2581 (2000).
[5] T. Cuk *et al.*, Phys. Rev. Lett. **93**, 117003 (2004).
[6] P. D. Johnson *et al.*, Phys. Rev. Lett. **87**, 177007 (2001).
[7] A. Kaminski *et al.*, Phys. Rev. Lett. **86**, 1070 (2001).
[8] T. K. Kim *et al.*, Phys. Rev. Lett. **91**, 167002 (2003).
[9] T. Valla, Proc. SPIE **5932**, 593203 (2005).
[10] K. Byczuk *et al.*, Nat. Phys. **3**, 168 (2007).
[11] J. Graf *et al.*, Phys. Rev. Lett. **98**, 067004 (2007).
[12] W. Meevasana *et al.*, Phys. Rev. B **75**, 174506 (2007).
[13] D. N. Basov and T. Timusk, Rev. Mod. Phys. **77**, 721 (2005).
[14] Y. S. Lee *et al.*, Phys. Rev. B **72**, 054529 (2005).
[15] D. van der Marel *et al.*, Nature (London) **425**, 271 (2003).
[16] M. B. J. Meinders *et al.*, Phys. Rev. B **48**, 3916 (1993).
[17] S. W. Moore *et al.*, Phys. Rev. B **66**, 060509(R) (2002).
[18] S. L. Cooper *et al.*, Phys. Rev. B **41**, 11605 (1990).
[19] S. Uchida *et al.*, Phys. Rev. B **43**, 7942 (1991).
[20] J. Bouvier *et al.*, Phys. Rev. B **45**, 8065 (1992).
[21] E. Dagotto, Rev. Mod. Phys. **66**, 763 (1994).
[22] J. Lorenzana and G. A. Sawatzky, Phys. Rev. Lett. **74**, 1867 (1995).
[23] J. Lorenzana and G. A. Sawatzky, Phys. Rev. B **52**, 9576 (1995).
[24] A. J. Leggett, Proc. Natl. Acad. Sci. U.S.A. **96**, 8365 (1999).
[25] M. Turlakov and Anthony J. Leggett, Phys. Rev. B **67**, 094517 (2003).
[26] V. J. Emery and S. A. Kivelson, Physica C **209**, 597 (1993).
[27] V. J. Emery and S. A. Kivelson, Phys. Rev. Lett. **74**, 3253 (1995).
[28] R. G. Leigh *et al.*, Phys. Rev. Lett. **99**, 046404 (2007).
[29] T.-P. Choy *et al.*, Phys. Rev. B **77**, 014512 (2008).
[30] T.-P. Choy *et al.*, Phys. Rev. B **77**, 104524 (2008).
[31] A. Georges *et al.*, Rev. Mod. Phys. **68**, 13 (1996).
[32] G. Kotliar *et al.*, Phys. Rev. Lett. **87**, 186401 (2001).
[33] T. D. Stanescu and G. Kotliar, Phys. Rev. B **74**, 125110 (2006).
[34] M. Jarrell *et al.*, Phys. Rev. B **51**, 11704 (1995).
[35] M. J. Rozenberg *et al.*, Phys. Rev. Lett. **75**, 105 (1995).
[36] M. M. Zemljič and P. Prelovšek, Phys. Rev. B **72**, 075108 (2005).
[37] K. Haule and G. Kotliar, Europhys. Lett. **77**, 27007 (2007); Phys. Rev. B **76**, 104509 (2007).
[38] H. Eskes *et al.*, Phys. Rev. B **50**, 17980 (1994).
[39] A. Comanac *et al.*, Nat. Phys. **4**, 287 (2008).
[40] A. Khurana, Phys. Rev. Lett. **64**, 1990 (1990).